Chemistry Europe
European Chemical Societies Publishing

WILEY VCH

Excellence in Chemistry Research

Announcing our new flagship journal

- Gold Open Access
- Publishing charges waived
- Preprints welcome
- Edited by active scientists

Meet the Editors of *ChemistryEurope*

Luisa De Cola
Università degli Studi di Milano Statale, Italy

Ive Hermans
University of Wisconsin-Madison, USA

Ken Tanaka
Tokyo Institute of Technology, Japan

Batteries & Supercaps

Research Article
doi.org/10.1002/batt.202300322

Chemistry Europe
European Chemical Societies Publishing

www.batteries-supercaps.org

Special Collection

Influences on Reliable Capacity Measurements of Hard Carbon in Highly Loaded Electrodes

Cedric Müller,[a] Zhengqi Wang,[a] Andreas Hofmann,[a] Pirmin Stüble,[a] Xinyang Liu-Théato,[a] Julian Klemens,[b] and Anna Smith*[a]

For the development of a full-cell battery system, typically appropriate cathodes and anodes are characterized within a half-cell setup where a metal counter electrode is installed to gather data about the employed electrodes. Ultimately, the individual capacity loadings allow for suitable balancing of the anode to cathode capacity in the full-cell. This approach seems rather unproblematic for lithium-ion batteries. For sodium-ion batteries, however, we show that the high reactivity of sodium metal strongly influences hard carbon-based electrode measurements within sodium-ion half-cells. As hard carbon is considered state-of-the-art anode material, the presented results have high impact on the development of sodium ion batteries. Specifically, we show that the type of electrolyte, as well as cell- and measurement-setup are key factors for reliable sodium half-cell measurements of hard carbon. The investigated hard carbon electrodes have a high active material loading of 7.2 mg/cm^2 (with 93% active material content) resulting in an areal capacity of 2.4 mAh/cm^2, which represent application-relevant conditions.

Introduction

The use of traditional energy sources and its consequences for the global climate is a well-investigated issue.[1] Therefore, power that is generated from fossil fuels is increasingly being replaced by renewable energy sources.[2] Driven by this development, batteries attract attention since they can be implemented in electric vehicles and in stationary energy storage systems to balance the unsteady energy supply from solar and wind power.[3] To meet the specific requirements for different applications, various cell chemistries are used for the electrochemical energy storage. Apart from established lithium-based cell chemistries, post-lithium systems can be a viable alternative to provide sufficient storage capacity for the growing market. Particularly, for lower range electric vehicle applications or stationary systems, where volumetric and/or gravimetric energy density can be accepted to be lower than state-of-the-art LIB's technology, sodium-ion batteries (NIBs) might act as a reasonable and potentially more sustainable complement.[4,5] The working principle of NIBs is similar to LIBs with supposedly analogue manufacturing conditions, e.g. electrode and cell manufacturing, thus NIB technology is considered as a drop-in technology for the already established production chain of LIBs.[6]

Currently, Prussian blue and manganese-based CAMs are considered the most promising cathode materials.[5] With a high specific capacity of about 300–335 mAh/g,[7,8] hard carbon (HC) is the most promising anode material for sodium-ion battery technology.[9] To investigate the electrochemical properties of the latter, half-cell measurements (working electrode vs. elemental metal sodium) are conducted. These experiments allow, for instance, to determine practical areal capacities and thus results are used to develop suitable electrode balancing (capacity ratio of anode to cathode or N/P) for full-cell systems.[7,10,11] A general challenge of half-cell measurements inserting elemental sodium is its reactivity not only towards oxygen and moisture, but also with different organic solvents used for electrolytes. If any component of the electrolyte is reacting with the sodium counter electrode over time, its surface is not stable during cycling and, thus, the recorded electrochemical behavior is influenced.[12]

Another pivotal issue when setting up two electrode half-cell measurements is the arising overpotential of sodium, which prevents an accurate control of the experiment via cell voltage. This phenomenon of polarization in sodium-ion half-cell measurements depends on the components of the electrolyte and was observed for ethylene carbonate (EC)-propylene carbonate (PC)-based electrolyte during cycling before.[13] Additives like fluoroethylene carbonate (FEC) can result in polarization in half-cell measurements, too.[14] To solve the issue

[a] C. Müller, Dr. Z. Wang, Dr. A. Hofmann, Dr. P. Stüble, Dr. X. Liu-Théato, Dr. A. Smith
Karlsruhe Institute of Technology (KIT)
Institute for Applied Materials (IAM)
Hermann-von-Helmholtz-Platz 1, 76344 Eggenstein-Leopoldshafen (Germany)
E-mail: anna.smith@kit.edu
Homepage: http://www.iam.kit.edu/ess/english/index.php

[b] J. Klemens
Karlsruhe Institute of Technology (KIT)
Institute for Applied Materials (IAM)
Straße am Forum 7, 76131 Karlsruhe (Germany)

Supporting information for this article is available on the WWW under https://doi.org/10.1002/batt.202300322

Special Collection This publication is part of a joint Special Collection dedicated to Post-Lithium Storage, featuring contributions published in Advanced Energy Materials, Batteries & Supercaps, and ChemSusChem.

Research Article
doi.org/10.1002/batt.202300322
Chemistry Europe
European Chemical Societies Publishing

of polarization in two electrode half-cells, it is highly necessary to employ a three-electrode setup.[15,16]

Within this paper we present the development of a reliable three electrode T-cell setup and measurement protocol to properly characterize highly loaded (meaning an areal capacity of >2 mAh/cm^2) hard carbon electrodes. A systematic electrolyte screening was performed to find the most stable electrolyte against elemental sodium preventing side reactions. Next, the effect of inappropriate vs. appropriate electrolytes on the electrochemical data obtained from T-cell half-cells (working electrode HC//sodium metal counter electrode with sodium metal reference electrode) is discussed and reproducibility and reliability of data is contrasted. Further, the impact of different control voltages (working electrode against counter vs. reference electrode) for the measurement set-up is demonstrated. Overall, the outcome of our study is that reliable and reproducible data is obtained for highly loaded HC electrodes in half-cells, if the electrolyte 1 M sodium hexafluorophosphate ($NaPF_6$) in EC:PC (1:1, w:w) with 5 wt% FEC is used and voltage readings are used from the potential difference of working electrode and current-free reference sodium metal (need of T-cell configuration). Thereby, polarization effects of sodium are minimized. Also using this setup, the cut-off potential at typically ~5 mV (close to 0 V) against Na/Na^+ during sodiation of HC is reached without premature shut-off allowing for full sodiation of HC before cut-off criteria are reached falsely. On the other hand, when controlling the voltage based on potential difference between working electrode and sodium metal counter electrode (as it is the typical case within simple coin cells), small variations of the reacting current-afflicted counter electrode lead to falsified potential readings and with HC having substantial capacity within the lower range of the voltage area, falsified, irreproducible and too small capacity readings are obtained.[15,17] Particularly, with increasing current and probably with increasing mass loading of HC this leads to even more falsified data. Our presented measuring cell setup has direct and high impact on the development of NIB full-cell systems, as proper capacity readings of cathode and anode are mandatory to set up ideal cell balancing, as shown in a further study.[11] Too high N/P ratio will result in a loss of energy density because the excess hard carbon material is not utilized. Too low N/P ratio will result in sodium plating on the hard carbon due to the excess sodium ions that are released from the cathode during charging and cannot be incorporated by the hard carbon.

Experimental Section

Electrolyte screening

For the electrolyte screening, solvent blends were mixed inside the glove box and filled in vials, where they were stored over sodium. Propylene carbonate and mixtures (1:1, w:w) of PC with either dimethyl carbonate (DMC), dimethoxyethane (DME), ethylene carbonate, ethylene glycol dimethyl ether (G1), tetraethylene glycol dimethyl ether (G4) or sulfolane (SL) were prepared. These solvents were used to prepare a 1 M solution of sodium hexafluorophosphate in a graduated flask. Lastly, 3 wt% fluoroethylene carbonate were added to some of the electrolytes. An overview of all electrolyte mixtures is given in Table 1. Photographs of the electrolytes with sodium metal pieces were taken after 130 days of storage (cf. Figure 1).

Gas chromatography (GC)

Gas chromatographic experiments were carried out using a Clarus 690 gas chromatograph from PerkinElmer Inc. that was equipped with an autosampler, a flame ionization detector (FID) and a mass spectroscopy (MS) detector (SQ 8T). The following parameters were used for the measurement as described elsewhere in detail:[18] He 6.0 (Air Liquide), H_2 gas from hydrogen generator (PG+160, Vici DBS), synthetic air (Air Liquide); Optima 5MS, 30 m length ×0.25 mm inner diameter, 0.5 μm path length; split flow of 20 mL/min, inlet temperature of 250 °C, 0.5 μL injection volume, 175 kPa initial pressure, pressure controlled mode, oven temperature 40 °C; oven and pressure parameters: 40 °C for 1.5 min, heating at 20 °C/min to 320 °C; pressure from 175 kPa for 2 min, rising at 7.8 kPa/min to 300 kPa. The MS setup was used as follows: filament voltage of 70 kV, ion source temperature of 200 °C, MS transfer line temperature of 200 °C, and the FID was run with following settings: 450 mL/min gas flow for synthetic air, 45 mL/min gas flow for hydrogen gas, FID temperature of 280 °C. Gas flow at the end of the separation column was divided by a SilFlow™ GC Capillary Column 3-port splitter to capture signals in both the MS and FID. The MS was used in scan mode with a scan range (33 u to 350 u) and the signals from the FID were used to determine the peak area. The software packages Turbomass 6.1.2 and OriginLab 2021b were used for data acquisition and data analysis.

For GC measurements sample preparation was conducted as follows: 25 μL of the respective electrolyte were mixed with 1.5 mL dichloromethane (CH_2Cl_2). After 30 minutes, the mixture was centrifuged, filtered and placed into the autosampler of the gas chromatograph (in total four different samples from one electrolyte mixture: 2× concentrated and 2× diluted with CH_2Cl_2 in 1:1 (v:v) ratio). The measurements were carried out after 30 days and 130 days of storage.

Table 1. Overview of the investigated electrolytes.

solvent	solvent composition	additive	conducting salt
PC	–	–	1 M $NaPF_6$
PC	–	3 wt% FEC	1 M $NaPF_6$
PC+DMC	50/50 (w/w)	–	1 M $NaPF_6$
PC+DMC	50/50 (w/w)	3 wt% FEC	1 M $NaPF_6$
PC+DEC	50/50 (w/w)	–	1 M $NaPF_6$
PC+DEC	50/50 (w/w)	3 wt% FEC	1 M $NaPF_6$
PC+EC	50/50 (w/w)	–	1 M $NaPF_6$
PC+EC	50/50 (w/w)	3 wt% FEC	1 M $NaPF_6$
PC+G1	50/50 (w/w)	–	1 M $NaPF_6$
PC+G1	50/50 (w/w)	3 wt% FEC	1 M $NaPF_6$
PC+G4	50/50 (w/w)	–	1 M $NaPF_6$
PC+G4	50/50 (w/w)	3 wt% FEC	1 M $NaPF_6$
PC+SL	50/50 (w/w)	–	1 M $NaPF_6$
PC+SL	50/50 (w/w)	3 wt% FEC	1 M $NaPF_6$

Research Article
doi.org/10.1002/batt.202300322
Chemistry Europe
European Chemical Societies Publishing

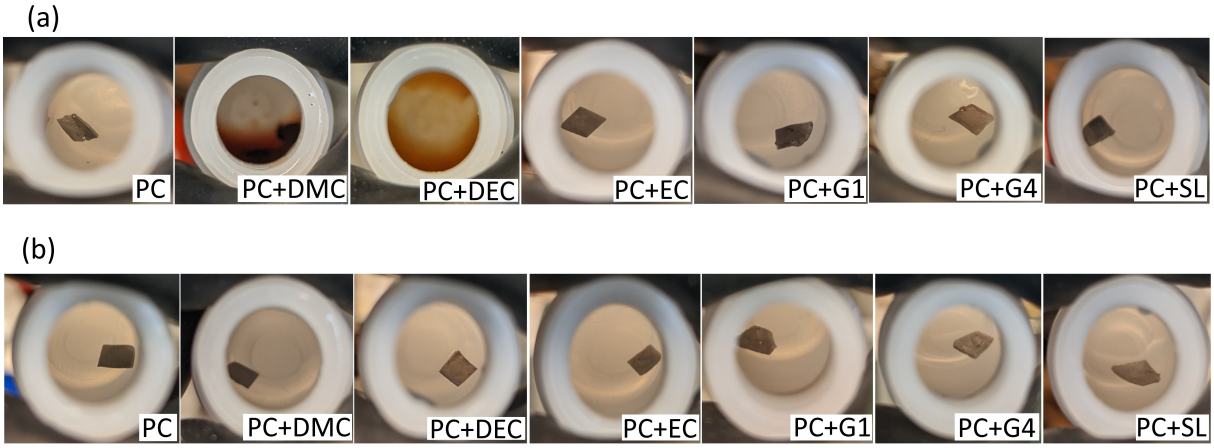

Figure 1. Optical images of vials containing different electrolyte in the presence of sodium metal after 130 d of storage without a) and with b) FEC as electrolyte additive.

Hard carbon electrode preparation and cell assembly

Hard carbon (Kuranode Type II, 9 μm average particle size, Kuraray) was coated onto aluminum foil (20 μm thickness, provided by Schlenk). According to a previously established formulation,[19] the slurry contained 93 wt% active material, 3.73 wt% styrene butadiene rubber (Zeon), 1.87 wt% carboxymethyl cellulose (MAC 500 LC, Nippon Paper), 1.4 wt% conductive carbon black powder (Timcal C-NERGY Super C65, Imersy) and was based on deionized water as a solvent. The coating had a thickness of 93 ± 2 μm and was calendered (roll at 50 °C) to a thickness of 83 ± 1 μm. An image taken with a Scanning Electron Microscope (SEM) of the calendered HC electrode is shown in Figure S1. Hard carbon electrodes, which were used as working electrodes, were punched out with a handheld precision punch tool (Nogamigiken Co., Japan), with a diameter of Ø = 12 mm. After drying, the loading of the electrodes was determined for each cell individually. The average active material loading was found to be 7.2(1) mg/cm^2. For the counter electrodes, sodium metal disks were freshly prepared inside the glovebox (argon atmosphere, water < 0.1 ppm, oxygen < 0.1 ppm). Sodium (Alfa Aesar, 99.8 %) was rolled between two plastic foils to a thickness of 1 mm. Electrodes with a diameter of 11 mm were then punched out for the use as counter electrode in the Swagelok cells. For fabrication of the reference electrodes, sodium was manually pressed into a plastic (made of PEEK) sleeve of the Swagelok cell. The cylindrical plastic sleeve can be loaded with sodium metal from one side and on the other side it has a circular hole with a diameter of 1 mm, which represents the surface of the resulting reference electrode, where sodium metal is sticking out. The other side is in contact with a steel stamp for electric connection.

To prepare the electrolyte for the cell tests, EC (Sigma Aldrich, 99 %) was firstly melted and then mixed with PC (Sigma Aldrich, 99.7 %) in a ratio of 1 : 1 (w : w). A 1 M $NaPF_6$ (Alfa Aesar, 99 %) solution was prepared in a volumetric flask. Finally, 5 wt% FEC (Sigma Aldrich, 99 %) were added. 500 μL of this electrolyte solution were inserted into each cell.

T-type Swagelok cells were used for three-electrode measurements. A photograph of the cell with the assignment of working, reference and counter electrode is shown in Figure S2. Cells were assembled in the glove box. The HC working electrodes were dried at 80 °C overnight and separators were dried at 120 °C under reduced pressure overnight. Three glass fiber separators (GF/D, Whatman) with a diameter of 13 mm were used for each cell. Two separators were placed between working electrode and counter electrode, one separator was placed in front of the reference electrode. Before cycling, the cells rested overnight at room temperature.

Electrochemical measurements

Electrochemical measurements were performed in a climate chamber at 25 ± 0.1 °C using a VMP-3 potentiostat (Biologic) with the EC-Lab software. The cells were cycled in the voltage range of 5 mV to 2 V vs. Na^+/Na. The detailed test protocol for the main investigation is shown in Table 2. For the formation, the cells were cycled at 0.05 C controlled by the potential between working and counter electrode for four cycles (step 1). Asymmetric rate capability tests were then conducted with different charging C-rates at 0.1 C, 0.2 C, 0.5 C, 1 C, 2 C, and back to 0.1 C finishing with a constant voltage-phase (cut-off at I < 0.05 C). The discharging C-rate was kept constant at 0.05 C for all cycles. At each C-rate, the cells were cycled twice. Two different voltage measuring methods were applied: the voltage cut-off was either controlled based on the potential difference of the working electrode against the reference electrode (step 2–7) or working electrode against counter electrode (step 8–13). This was done to investigate the influence of the used control voltage on the data obtained. Finally, two cycles charged at 0.1 C constant current, and subsequent constant voltage (until $I < 0.05$ C) and discharged at 0.05 C were conducted where voltage measurement was performed between working and reference electrode.

In addition, according to Table 3, the formation was repeated on a set of newly prepared cells, where voltage control was performed by the potential difference of working electrode to reference electrode.

Statistical analysis of cell data

Four Swagelok cells were built for each experiment. Of these, often one, and sometimes even two cells showed obvious malfunctions. For instance, expected charge and discharge capacities were not achieved by far or significantly accelerated degradation occurred. Overall, the measurement data with the control voltage vs. counter electrode show a stronger variability than data generated by using the control voltage vs. reference electrode. The data given in this study and its figures in each case represent the results of the cell with the best performance. In all cases, however, the data are confirmed by at least one other measurement with a deviation of

Research Article
doi.org/10.1002/batt.202300322
Chemistry Europe
European Chemical Societies Publishing

Table 2. Detailed test protocol for T-cell measurements. Note that step 1 had pure CC steps for charging, while a CV-phase was applied for steps 2–14 using a cut-off current of 0.05 C.

step	number of cycles	first cycle	last cycle	charge rate	discharge rate	control voltage
1	4	1	4	0.05 C	0.05 C	HC vs. Counter electrode
2	2	5	6	0.1 C	0.05 C	HC vs. Reference electrode
3	2	7	8	0.2 C	0.05 C	HC vs. Reference electrode
4	2	9	10	0.5 C	0.05 C	HC vs. Reference electrode
5	2	11	12	1.0 C	0.05 C	HC vs. Reference electrode
6	2	13	14	2.0 C	0.05 C	HC vs. Reference electrode
7	2	15	16	0.1 C	0.05 C	HC vs. Reference electrode
8	2	17	18	0.1 C	0.05 C	HC vs. Counter electrode
9	2	19	20	0.2 C	0.05 C	HC vs. Counter electrode
10	2	21	22	0.5 C	0.05 C	HC vs. Counter electrode
11	2	23	24	1.0 C	0.05 C	HC vs. Counter electrode
12	2	25	26	2.0 C	0.05 C	HC vs. Counter electrode
13	2	27	28	0.1 C	0.05 C	HC vs. Counter electrode
14	2	29	30	0.1 C	0.05 C	HC vs. Reference electrode

Table 3. Alternative protocol for the investigation of the cell formation.

step	number of cycles	first cycle	last cycle	charge rate	discharge rate	control voltage
1	4	1	4	0.05 C	0.05 C	HC vs. Reference electrode

less than 3% when cycling vs. reference electrode potential, or less than 10% when cycling vs. counter electrode potential.

Results and Discussion

Electrolyte selection

In this study, selected and commercially relevant electrolyte mixtures based on PC and $NaPF_6$ were examined for their chemical reactivity with sodium metal. A small screening test was performed to determine the most suitable electrolyte from the series. Namely, the solvent mixtures PC, PC + DMC, PC + DEC, PC + EC, PC + G1, PC + G4 and PC + SL (see Table 1 for detailed solvent mixture composition) were investigated towards their stability. The selection was based on literature screening and pre-tests where sodium perchlorate ($NaClO_4$) was used as the conducting salt.[18] PC was chosen as cyclic carbonate source due to its superior flow characteristics compared to EC and its compatibility with hard carbon used as anode materials in NIB. Both mixtures EC/DMC and EC/DEC, which can be expected to have a high reactivity with Na based on pre-screening tests,[18] were selected to demonstrate the influence of the additive FEC. EC, SL, G4 as well as SL exhibit high flash points which enhance the intrinsic electrolyte safety in terms of non-flammability.[20] FEC as an additive was chosen due to its widespread use in NIB in a concentration range between 1–5% and due to its improvement in the electrolyte degradation of solvent mixtures.[18]

In the first step, aging tests were carried out and the electrolyte-sodium metal mixtures were examined after 130 days of storage, see Figure 1(a) for optical images without FEC as an additive and Figure 1(b) with FEC as an additive. It can be observed that both mixtures PC + DMC and PC + DEC show considerable color changes when no FEC is present, whereas 3 wt% FEC in the electrolyte leads to a clear improvement and practically no discolorations are visible anymore, which is widely observed in literature.[21] With FEC, all mixtures stay colorless in the presence of sodium metal. This might be because FEC reacts with the sodium metal and the resulting surface hampers further electrolyte degradation.

After a storage time of 130 days, all mixtures were analyzed via gas chromatography to detect volatile compounds and decomposition products, which may have formed during storage. Exemplarily, two chromatograms are shown in Figure 2 for PC + DMC + $NaPF_6$ electrolyte, once with and once without FEC. It can clearly be observed that FEC reduces the formation of side products (less peaks are visible in the chromatogram). For instance, neither glyme derivatives (C, cf. Figure 2) nor DMC-PC coupling compound E (dimethyl propane-1,2-diyl dicarbonate, cf. Figure 2[18]) can be seen when FEC is present in the mixture at 3 wt% ratio. Such a trend can semi-quantitatively be described when referring the products to the total solvent amount (without FEC) in the mixture by comparing the FID peak area. It is found that the FEC content in the electrolyte is approximately 3 wt%, as expected due to its content. For direct comparison of all electrolyte mixtures, normalized FID areas for different decomposition products are displayed in Figure 3. The largest effect of FEC being used as an additive is observed

Research Article
doi.org/10.1002/batt.202300322
Chemistry Europe
European Chemical Societies Publishing

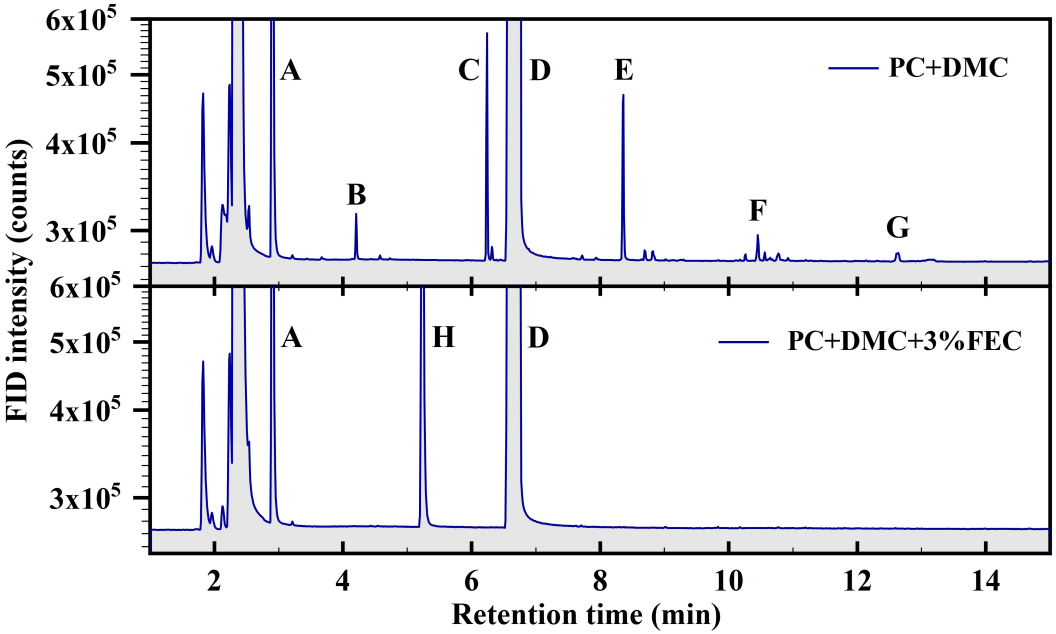

Figure 2. Exemplary chromatograms of solvent mixture after 130 d of storage over sodium metal: a) PC + DMC + $NaPF_6$, b) PC + DMC + FEC + $NaPF_6$. Assignment of peaks: A = DMC, B = isopropyl methyl carbonate (NIST), C = diethylene glycol diethyl ether, D = PC, E = dimethyl propane-1,2-diyl dicarbonate,[18] F = unknown, G = unknown, H = FEC "(NIST)": The most likely substance was determined based on a NIST comparison only.

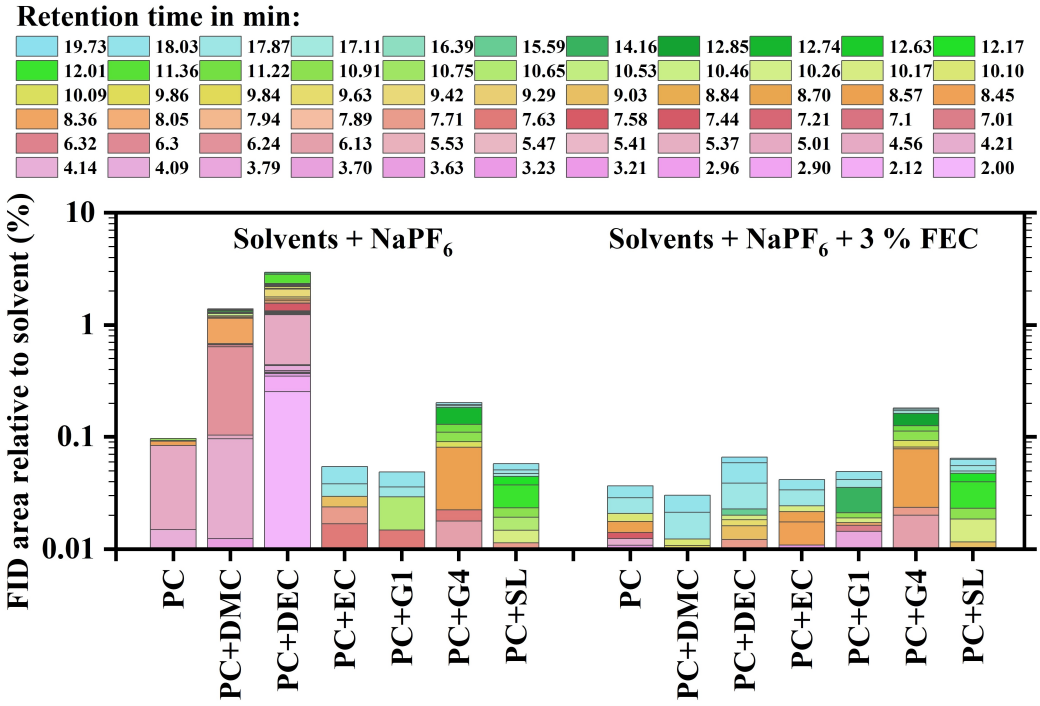

Figure 3. Semi-quantitative analysis of decomposition products found in GC analysis of electrolyte mixtures stored over sodium metal for 130 d. The diagram does not include the main solvent components. All peaks were related to the relative area ratio referred to the total electrolyte solvent.

when linear and cyclic carbonates are used within the mixture, e.g., PC + DMC or PC + DEC. In this case, FEC reduced the side reactions significantly. In contrast, FEC has no obvious effect on the formation of decomposition products in the case of PC + G4 and PC + SL electrolytes. For PC and PC + EC, minor effects are observed in the liquid electrolyte. Nevertheless, it can be seen, that the formation of longer/larger products (e.g., oligomers) is more favorable when FEC is present. Such compounds, formed between electrolyte and sodium metal by surface reactions, can be dissolved from the sodium metal surface into the electrolyte if sufficiently soluble. In Figure 3, the retention times (RT) of the detected compounds are mentioned as well in order to

distinguish between relatively short molecules (small RT, e.g., carbonates, ethers) and longer chain products (e.g., oligomers). The *n*-alkanes can serve as a reference point, longer alkanes (C15–C20) exhibit retention times of 10.5–16.0 min, and the blue colored compounds from Figure 3 complies to n-alkanes of C22–C24 chain length. Based on the experiments and literature results of glyme compounds, which result in strong sodium metal surface reactions,[18] the mixture PC + EC + $NaPF_6$ was identified as most promising electrolyte formulation for the study. In this case, even without FEC as additive very few pronounced formation of soluble decomposition products are formed.

Figure 4 shows both sets of chromatograms of PC + EC with $NaPF_6$ and with and without FEC, respectively. EC and PC appeared as one peak (A) and FEC is visible in Figure 4 at a retention time of 5.25 min. Apart from the main bands of FEC, EC and PC, only traces of impurities are visible. This is expressed by the very low impurity in Figure 3. In this context, it should be noted that the *y*-scale of Figure 3 is shown logarithmically. The bands in the range 1.8–2.6 min are assigned to solvents and gases that do not originate directly from the sample. Due to the main scope of the study in terms of three electrode measurements of NIB, the pre-screening of the electrolytes is done and shown to evaluate suitable electrolyte formulations and to demonstrate the positive effect of FEC regarding electrolyte decomposition. The detailed investigation of the decomposition pathways and products formed on the surface of the electrodes and sodium metal is therefore beyond the scope of this work.

Cell testing

For half-cell measurements of highly loaded hard carbon electrodes (7.2 mg/cm^2, 93% active material) 1 M $NaPF_6$ in EC:PC (1:1, w:w) with 5 wt% FEC (electrolyte A) was selected for cell testing, because in the previous electrolyte study 1 M $NaPF_6$ in EC:PC (1:1, w:w) with 3 wt% FEC turned out to be the most stable electrolyte composition towards elemental sodium among the investigated electrolytes. FEC is reported to stabilize the sodium metal electrolyte interphase, while it is also consumed in NaF rich solid electrolyte interphase (SEI) formation on the HC.[18,22] To counteract the loss of FEC and to assure that a sufficient quantity of FEC remains in the electrolyte, 5 wt% instead of 3 wt% FEC were used. The slightly higher concentration was chosen because of the consumption of FEC. At the same time, it was observed that higher concentrations (e.g., 10%) do not result in any improvement, but rather lead to a deterioration of cell performance. On the other side, 1 M $NaPF_6$ in PC:DMC (1:1, w:w) (electrolyte B) was determined as the least stable electrolyte composition towards elemental sodium. The cell testing was carried out with both electrolytes in order to investigate the influence of the stability of different electrolyte compositions on resulting cell test data.

Within this study, T-cells were used, where the three-electrode setup enables the use of two different control voltages. From here on "cycling vs. counter electrode voltage" is referred to when the voltage reading results from the potential difference between working electrode (HC) and the counter electrode (sodium metal). Despite the fact, that one can monitor the individual half-cell voltages, this setup corresponds to any traditional two-electrode measurement, like e.g., in coin cells. "Cycling vs. reference electrode voltage", in contrast requires a reference electrode. Here, the voltage measurement

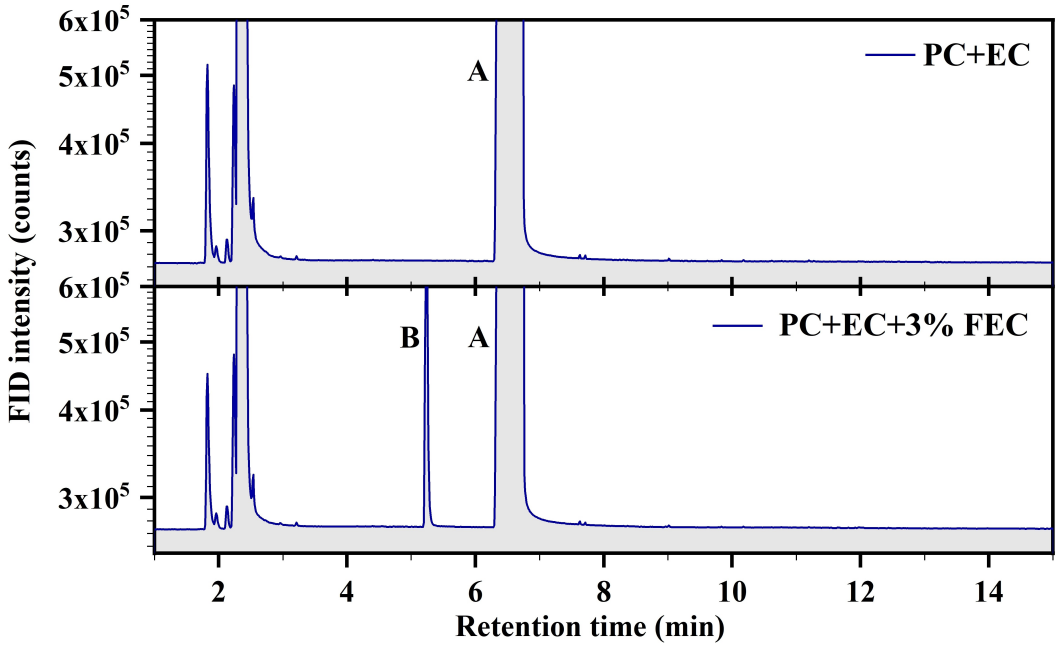

Figure 4. Chromatograms of a) EC + PC + $NaPF_6$ and b) EC + PC + FEC + $NaPF_6$ electrolyte after 130 d storage over sodium metal. A = PC, B = FEC "(NIST)": The most likely substance was determined based on a NIST comparison only.

Research Article
doi.org/10.1002/batt.202300322
Chemistry Europe
European Chemical Societies Publishing

is the potential difference of the working electrode (HC) against the reference electrode (sodium metal), which is free of current being applied. Instead, current only passes through the counter electrode (sodium metal). Within this setup, the difference between sodium metal reference and sodium metal counter electrode can be monitored. All tests were performed within the voltage window of 0.005–2 V vs. Na^+/Na.

The formation cycles displayed in Figure 5(a and b) were conducted vs. counter electrode voltage. It can be seen that with the electrolyte A, which is actually well suited for the system in terms of sodium metal degradation, the charge and with that its subsequent discharge capacity of the electrode is underestimated. The discharge capacity is found to be 242 mAh/g in the first cycle and decreases to 230 mAh/g in the fourth cycle (cf. Figure 5a). This can probably be directly attributed to FEC related cell polarization.[14] Since the formation of SEI interfaces also affects polarization, a changed SEI composition due to the addition of FEC can also have an impact on discharge capacity. In each cycle, the charging step seems pre-maturely terminated before the complete sodiation of HC and, accordingly, less sodium is available during the discharge step. This issue apparently does not occur with electrolyte B, where discharge capacities vary between 259 mAh/g and 272 mAh/g. Accordingly, it seems that the electrolyte stability does not negatively influence the electrochemical performance of the first cycles. Despite multiple experiments, the formation cycles vs. counter electrode potential and its coulombic efficiencies (CE) varied unreliably.

The formation shown in Figure 5(c) was conducted vs. reference electrode voltage with electrolyte A. The measurements of all four cells delivered reliable data with a deviation of less than 1% for the initial coulombic efficiencies (ICE). The initial charge capacity for the cell displayed in Figure 5(c) was 335 mAh/g and the initial discharge capacity was 265 mAh/g. As a result, the initial coulombic efficiency (ICE) of HC was 79%. The following cycles delivered a reversible capacity of 265 mAh/g with a CE of 98–99%. This represents a reliable measurement regarding the charge/discharge capacity and the ICE of HC anodes with a loading of 2.4 mAh/cm^2, which is an important milestone to investigate and to optimize HC electrodes. The accurate knowledge of the capacity of HC electrodes allows for proper balancing of corresponding cathodes, as show in an additional work on $Na_3V_2(PO_4)_3$/C vs. HC full cells with a decent cycling stability and cathode loadings of 1.2 mAh/cm^2.[11] Cathodes with specific capacity of ~2 mAh/cm^2 have likewise been developed and are currently being tested in combination with the HC electrode investigated herein.

After formation vs. counter electrode potential, two consecutive asymmetric rate capability tests were conducted with various charge rates at 0.1 C, 0.2 C, 0.5 C, 1 C and 2 C, followed by 0.1 C to verify possible degradation during charging (all charge steps finished with a constant voltage phase, until $I <$ 0.05 C). Discharge was performed using a rate of 0.05 C. The first rate capability test was controlled vs. reference electrode voltage (see Figure 6). This control voltage was chosen in order to avoid possible influences of the current-carrying sodium counter electrode on the potential-driven cycling.

The cell was charged via a CC phase until the cut-off potential of 5 mV between the HC working electrode and the sodium reference electrode was reached. A constant voltage (CV) phase followed, where a potential of 5 mV between working electrode and reference electrode was applied until the current decreased below 0.05 C. The CV phase for charging was added to achieve the total available charge capacity of the HC anodes.

While the charge, and therefore respective discharge, capacities with electrolyte B were decreasing to less than 70 mAh/g during cycling (cf. Figure 6b), the cells with electrolyte A delivered stable charge and corresponding discharge capacities of 265 mAh/g (cf. Figure 6a).

The different capacities obtained with both electrolyte compositions can be explained by different stabilities towards the sodium metal counter electrode. Side reactions, here for electrolyte B, result in electrolyte degradation, that have been observed in chapter 3.1, and lead to a blocked surface of the sodium counter electrode just by storage contact. After cycling with electrolyte B was completed, the counter electrode was extracted from the cell and the surface of sodium was inspected showing severe crud formation (cf. Figure S3). In accordance, GC analysis of the extracted electrolyte B after cycling show more degradation products and larger amounts compared to storage over sodium metal (cf. Figure S4). This might explain, why control of the cell voltage was falsified such that the 5 mV HC against Na/Na^+ of the reference was not given. Most likely

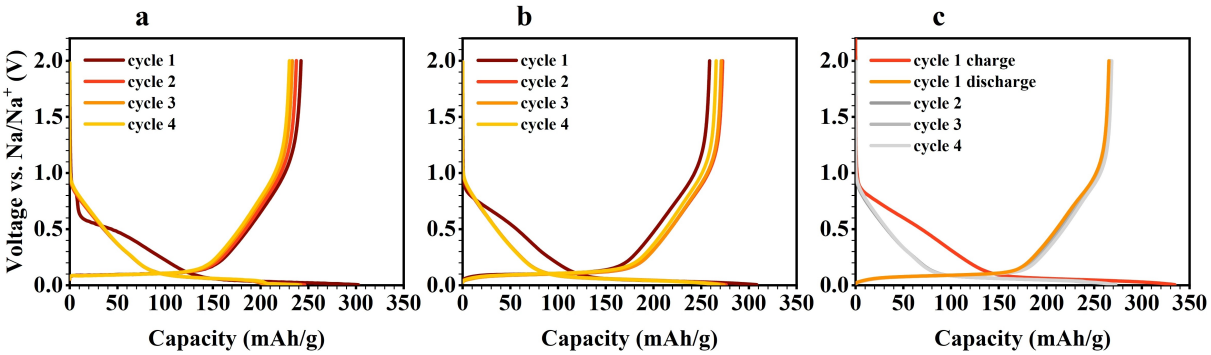

Figure 5. Potential curves for the formation cycles at 0.05 C of hard carbon vs. counter electrode voltage: a) 1 M $NaPF_6$ in EC:PC (1:1) with 5 wt% FEC, electrolyte A, and b) 1 M $NaPF_6$ in PC:DMC (1:1), electrolyte B. Formation vs. reference electrode voltage: c) 1 M $NaPF_6$ in EC:PC (1:1) with 5 wt% FEC.

Research Article
doi.org/10.1002/batt.202300322
Chemistry Europe
European Chemical Societies Publishing

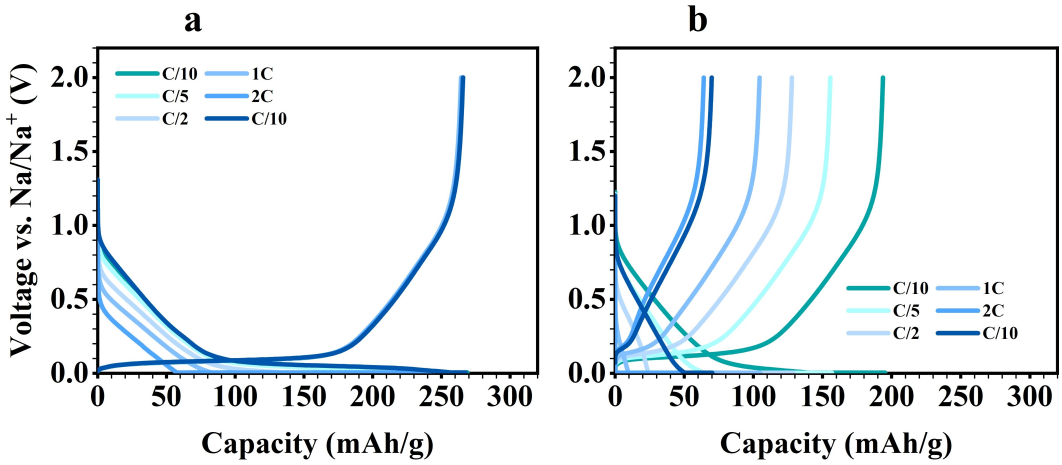

Figure 6. Charge rate performances of HC in half-cells controlled vs. reference electrode voltage: a) 1 M $NaPF_6$ in EC:PC (1 : 1) with 5 wt% FEC and b) 1 M $NaPF_6$ in PC:DMC (1 : 1). Two cycles per C-rate were conducted with only the second cycle being displayed.

the cell was shut-off pre-maturely, leading to incomplete sodiation of HC during charge. It is also possible that the surface of the sodium metal counter electrode was blocked (ionic or electric insulation) resulting in insufficient stripping and plating performance of the counter electrode.

The second rate capability test was performed analogously, with the difference that it was controlled vs. the cell voltage instead of the half-cell voltage. The results are displayed in Figure 7. Possibly due to the previously described electrolyte stability towards the sodium metal electrode, the half-cell with electrolyte B had lost most of its capacity, with only about 27 mAh/g left (cf. Figure 7b).

However, the half-cell with electrolyte A delivered higher, but continuously decreasing discharge capacities (cf. Figure 7a). At the beginning and at the end of this rate capability test, two cycles at a C-rate of 0.1 C were conducted. While the first cycle showed discharge capacities of 234 mAh/g, the cycle at the end ended up at 209 mAh/g (cf. Figure 7a). This difference of 25 mAh/g illustrates a decrease of capacity during cycling, which could indicate aging of the half-cell.

Compared to the values obtained from the previous rate capability test vs. reference electrode, the rate capability test vs. counter electrode resulted in significantly lower and also continuously decreasing capacities. The initial decrease by 31 mAh/g, from 265 mAh/g to 234 mAh/g, originates from the swap of control voltage from reference electrode potential to counter electrode potential. Therefore, the measurements show the effect of the potential difference of current-carrying sodium at the counter electrode and currentless sodium at the reference electrode during cycling. This potential difference corresponds to a shifted potential that indicates an electrochemical change of the counter electrode through cycling. This shift of the sodium metal counter electrode potential in half-cell measurements distorts any electrochemical investigations of electrode material on the side of the working electrode. In the case of HC, a significant amount of capacity is located at a low-voltage window. Hence, a shift of the potential that is used as

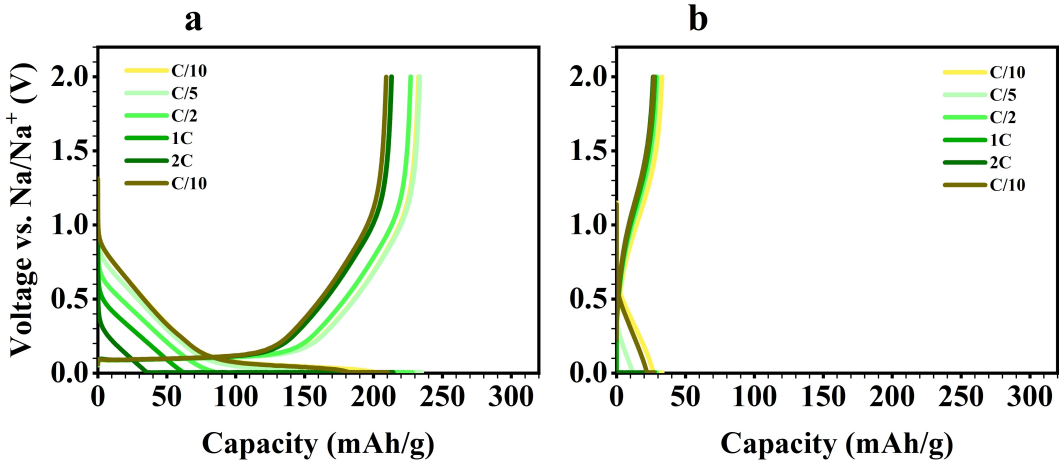

Figure 7. Charge rate performances of HC in half-cells controlled vs. counter electrode voltage: a) 1 M $NaPF_6$ in EC:PC (1 : 1) with 5 wt% FEC and b) 1 M $NaPF_6$ in PC:DMC (1 : 1). Two cycles per C-rate were conducted with only the second cycle being displayed.

Research Article
doi.org/10.1002/batt.202300322
Chemistry Europe
European Chemical Societies Publishing

the control voltage can have a crucial influence on the half-cell measurement of HC leading to falsified capacity readings. After the second rate capability test vs. counter electrode potential, two additional cycles at a C-rate of 0.1 C vs. reference electrode potential were conducted (cf. Figure S5). Although the half-cell with electrolyte A delivered only 209 mAh/g at the end of the previous rate capability test vs. counter electrode potential, the following cycles vs. reference electrode potential demonstrate discharge capacities of 258 mAh/g and 259 mAh/g (cf. Figure S5a), which are in the range of the initial capacities obtained vs. reference electrode potential. This shows the significant difference between the measuring method vs. reference electrode potential compared to vs. counter electrode potential. The half-cell with electrolyte B delivers about 24 mAh/g in both cycles (cf. Figure S5b). It can be assumed that the previously described processes keep decreasing the capacity.

Overall, the results displayed in Figures 6(b), 7(a and b) might be misleadingly interpreted as material degradation. However, showing all sets of data, it is clear that particularly for a proper capacity (retention) and performance measurement of HC within sodium-based half-cells, it is important to use stable electrolyte and proper cell measurement conditions (voltage control against a reference electrode).

For sake of completeness, results from previous chapters (including data from Figures 6, 7 and S5) are directly compared to each other: In Figure 8, the charge capacities of the two consecutive rate capability tests and of the two additional cycles with differing control voltages are illustrated. The results shown in this overview underline the influences of electrolyte degradation and of the control voltage.

To further evaluate the rate capability of the investigated HC electrode, it is reasonable to separately consider the capacity contributions of the CC-Steps and the CV-Steps, respectively. The effect that an increasing charge rate results in decreasing CC charge capacity is found unsurprisingly. The two charge capacities measured vs. reference electrode potential with electrolyte A at a C-rate of 0.5 C are 139 mAh/g and 134 mAh/g (cf. Figure 8a) which basically seem to be rather low values. This raises the question of whether, if these limits are exceeded, further CC charging would lead to the deposition of elemental sodium on HC side. To answer this question, additional three-electrode investigations with counter electrodes based on active materials like carbon-coated sodium vanadium phosphate are currently in preparation. It seems conceivable that due to the higher potential difference between working and counter electrode, different CC and CV fractions could be obtained for HC within a full-cell setup.

A HC electrode with a lower loading (4.3 mg/cm^2, 1.4 mAh/g) shows a similar rate capability indicating that the high loading does not affect the rate capability (cf. Figure S6). However, for other HC materials the C-rate-dependent limits of the CC-Step were observed.[9,23] In this respect, further research is undoubtedly needed.

In Figure 9, the charge (CC varied + CV (cut-off at 0.05 C) and the discharge (CC using 0.05 C) capacities of the two rate capability tests are shown. Beside the previously discussed charge capacities, the difference between charge capacity and discharge capacity is visualized. In the first cycles of the rate capability test vs. reference electrode voltage with electrolyte A (cf. Figure 9a), the coulombic efficiency is slowly increasing from 98.1 % to 99.3 %. This indicates that the SEI formation was not completed after four formation cycles vs. counter electrode potential, which directly shows the influence that the control potential can have. Furthermore, the coulombic efficiencies of the following cycles are about 99 % and show no irregularities. However, cycling with FEC typically results in slightly decreased CEs due to consumption and degradation of the additive.

While counter and reference electrode both consist of sodium metal, the difference of cycling vs. reference electrode voltage and vs. counter electrode voltage lies in a shift in the potential of the counter electrode by current flow on the supposition that the potential of the reference electrode remains constant. In Figure 10, the potential between the sodium counter electrode and the sodium reference electrode during the rate capability test vs. reference electrode potential

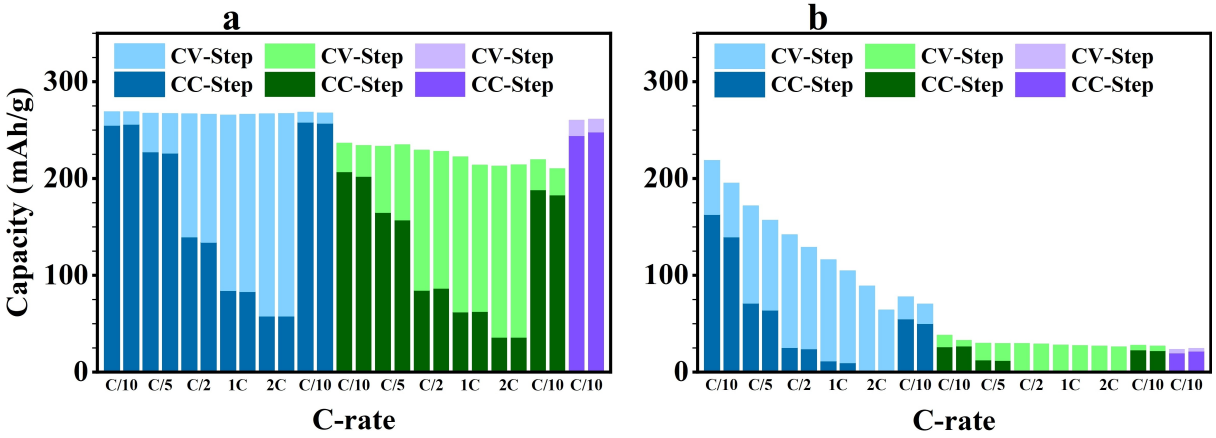

Figure 8. Charge capacities of the consecutive sequences including the ratio of charge provided from constant current (CC) phase and constant voltage (CV) phase: a) 1 M $NaPF_6$ in EC:PC (1 : 1) with 5 wt% FEC and b) 1 M $NaPF_6$ in PC:DMC (1 : 1). The charge rate capability test vs. reference electrode voltage is blue colored (cf. Figure 6), the charge rate capability test vs. counter electrode voltage is green colored (cf. Figure 7), and two conclusive cycles vs. reference electrode voltage are purple colored (cf. Figure S5).

Research Article
doi.org/10.1002/batt.202300322
Chemistry Europe
European Chemical Societies Publishing

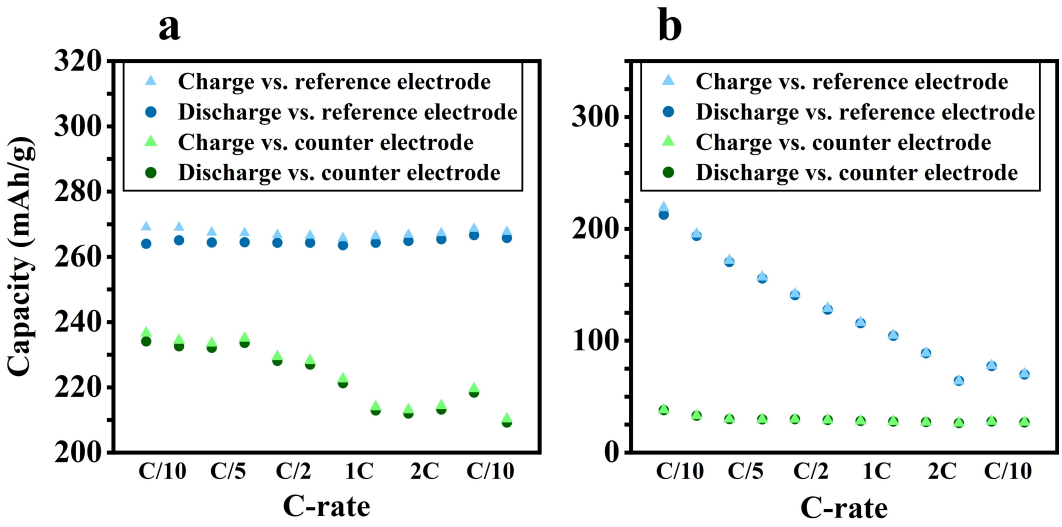

Figure 9. Comparisons of charge and discharge capacities of two consecutive rate capability tests: a) 1 M $NaPF_6$ in EC:PC (1:1) with 5 wt% FEC and b) 1 M $NaPF_6$ in PC:DMC (1:1). The charge rate capability test vs. reference electrode voltage performed first is shown in blue and the charge rate capability test vs. counter electrode voltage performed afterwards is shown in green.

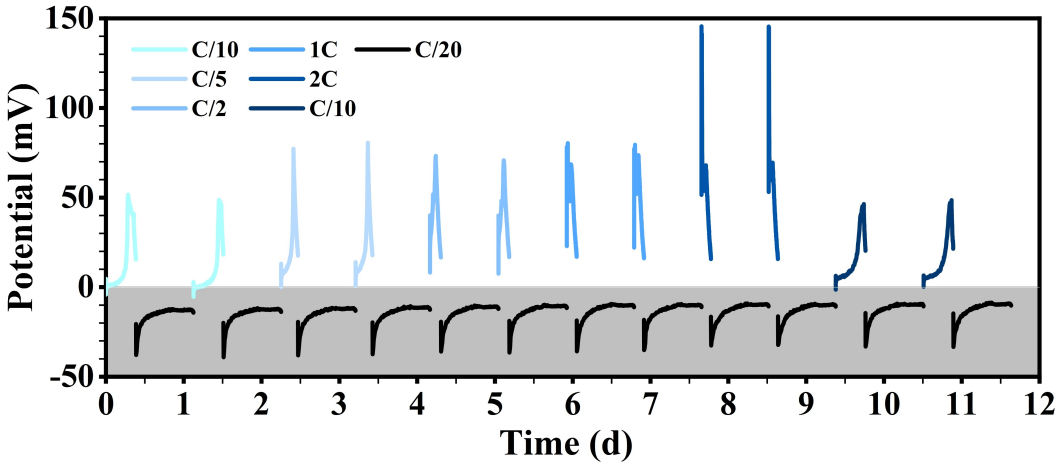

Figure 10. Potential between sodium counter electrode and sodium reference electrode during the charge rate capability test vs. reference electrode voltage with 1 M $NaPF_6$ in EC:PC (1:1) with 5 wt% FEC shown in Figure 6(a). The charging rates were varied and are shown in blue colors, the constant discharge rate of 0.05 C is black.

using electrolyte A (cf. Figure 6a) is illustrated. During charging the shift of the counter electrode potential vs. reference electrode potential is positive and during discharging it is negative. Also, it is dependent on the C-rate. The shift of the counter electrode potential vs. reference electrode potential is around 50 mV for various C-rates and increases up to 150 mV at 2 C. In conclusion, it has direct impact on the measurement when using measurement setup controlled vs. counter electrode potential.

Conclusions

Different $NaPF_6$-containig electrolyte compositions were used for storage aging tests over elemental sodium and the respective decomposition products comprising a vapor pressure investigated with gas chromatography. From these results, a stable electrolyte composition against sodium metal and an unstable electrolyte composition against sodium metal were determined and the influence of electrolyte decomposition on the cycling performance of HC half-cells was examined. Thereby, 1 M $NaPF_6$ in EC:PC (1:1, w:w) with 5 wt% FEC was found to be a suitable electrolyte composition for HC half-cell measurements against elemental sodium.

In contrast to previous studies, in which HC was investigated within thin electrodes with low active material content, it is shown how the capacity and rate dependent cycling behavior of highly loaded anodes with 93 wt.% HC and an areal capacity of 2.4 mAh/cm^2 can be properly investigated using a three-electrode setup. For all C-rates, controlling the charge and discharge steps based on the voltage of the working electrode (HC) vs. the sodium reference electrode yields in much more

reliable and reproducible data compared to experiments controlled via the voltage vs. the sodium counter electrode. The three-electrode setup, therefore, allows circumventing the issue of varying potentials of the current-carrying sodium counter electrode and thus allows trustworthy capacity readings of the HC electrodes. The proper balancing (N/P) within full cells, is crucial to avoid sodium plating and with that capacity degradation on the one hand, and increase of overall energy density of the cell on the other hand. Such optimal balancing is only possible when individual electrodes can be characterized reliably in terms of capacity readings.

From the rate capability test, it becomes apparent that for the highly loaded HC anode investigated herein, only about 50% of the capacity is accessible via the CC charging step at a moderate C-rate of 0.5 C. This raises the question whether the HC active material or the electrode composition need to be further optimized and improved in this respect in order to enable application in fast charging NIBs.

Acknowledgements

This work was funded by the Deutsche Forschungsgemeinschaft (DFG, German Research Foundation) under Germany's Excellence Strategy - EXC 2154 - Project number 390874152 (POLiS Cluster of Excellence), and contributes to the research performed at Center for Electrochemical Energy Storage Ulm Karlsruhe (CELEST). We would like to thank Dr.-Ing. Philip Scharfer and Prof. Dr.-Ing. Wilhelm Schabel from Thin Film Technology at KIT for coating and drying electrodes in their TFT Coating and Printing Lab within the scope of the joint research in the DFG Cluster of Excellence POLiS. Open Access funding enabled and organized by Projekt DEAL.

Conflict of Interests

The authors declare no conflict of interest.

Data Availability Statement

The data that support the findings of this study are available from the corresponding author upon reasonable request.

Keywords: sodium-ion battery · half-cell measurement · hard carbon · three-electrode cell · T-cell

[1] Contribution of Working Groups I, II and III to the Sixth Assessment Report of the Intergovernmental Panel on Climate Change (Core Writing Team, H. Lee and J. Romero (eds.)), *Climate Change 2023: Synthesis Report*, **2023**.
[2] International Energy Agency, *World Energy Outlook 2021*.
[3] a) S. Ould Amrouche, D. Rekioua, T. Rekioua, S. Bacha, *Int. J. Hydrogen Energy* **2016**, *41*, 20914; b) A. Eftekhari, *ACS Sustainable Chem. Eng.* **2019**, *7*, 5602; c) Y. Yang, S. Bremner, C. Menictas, M. Kay, *Renewable Sustainable Energy Rev.* **2018**, *91*, 109.
[4] a) M.-M. Titirici, *Adv. Energy Mater.* **2021**, *11*, 2003700; b) C. Vaalma, D. Buchholz, M. Weil, S. Passerini, *Nat. Rev. Mater.* **2018**, *3*, 18013.
[5] M. Baumann, M. Häringer, M. Schmidt, L. Schneider, J. F. Peters, W. Bauer, J. R. Binder, M. Weil, *Adv. Energy Mater.* **2022**, *12*, 2202636.
[6] a) J. Peters, A. Peña Cruz, M. Weil, *Batteries* **2019**, *5*, 10; b) M. Fichtner, *Batter. Supercaps* **2022**, *5*.
[7] D. A. Stevens, J. R. Dahn, *J. Electrochem. Soc.* **2000**, *147*, 1271.
[8] a) Z. Wang, X. Feng, Y. Bai, H. Yang, R. Dong, X. Wang, H. Xu, Q. Wang, H. Li, H. Gao et al., *Adv. Energy Mater.* **2021**, *11*, 2003854; b) D. Saurel, B. Orayech, B. Xiao, D. Carriazo, X. Li, T. Rojo, *Adv. Energy Mater.* **2018**, *8*, 1703268.
[9] F. Xie, Z. Xu, Z. Guo, M.-M. Titirici, *Prog. Energy* **2020**, *2*, 42002.
[10] a) H. Au, H. Alptekin, A. C. S. Jensen, E. Olsson, C. A. O'Keefe, T. Smith, M. Crespo-Ribadeneyra, T. F. Headen, C. P. Grey, Q. Cai et al., *Energy Environ. Sci.* **2020**, *13*, 3469; b) L. Xiao, H. Lu, Y. Fang, M. L. Sushko, Y. Cao, X. Ai, H. Yang, J. Liu, *Adv. Energy Mater.* **2018**, *8*, 1703238.
[11] Pirmin Stüble, Cedric Müller, Julian Klemens, Philip Scharfer, Wilhelm Schabel, Marcel Häringer, Joachim R. Binder, Andreas Hofmann, Anna Smith, *ChemRxiv* **2023**, preprint: DOI: 10.26434/chemrxiv-2023-jf6mq.
[12] K. Pfeifer, S. Arnold, J. Becherer, C. Das, J. Maibach, H. Ehrenberg, S. Dsoke, *ChemSusChem* **2019**, *12*, 3312.
[13] A. Rudola, D. Aurbach, P. Balaya, *Electrochem. Commun.* **2014**, *46*, 56.
[14] T. Akçay, M. Häringer, K. Pfeifer, J. Anhalt, J. R. Binder, S. Dsoke, D. Kramer, R. Mönig, *ACS Appl. Energ. Mater.* **2021**, *4*, 12688.
[15] Z. Li, Z. Jian, X. Wang, I. A. Rodríguez-Pérez, C. Bommier, X. Ji, *Chem. Commun. (Camb.)* **2017**, *53*, 2610.
[16] J. Fondard, E. Irisarri, C. Courrèges, M. R. Palacin, A. Ponrouch, R. Dedryvère, *J. Electrochem. Soc.* **2020**, *167*, 70526.
[17] a) Y. Zheng, Y. Wang, Y. Lu, Y.-S. Hu, J. Li, *Nano Energy* **2017**, *39*, 489; b) X. Chen, Y. Zheng, W. Liu, C. Zhang, S. Li, J. Li, *Nanoscale* **2019**, *11*, 22196.
[18] A. Hofmann, Z. Wang, S. P. Bautista, M. Weil, F. Müller, R. Löwe, L. Schneider, I. U. Mohsin, T. Hanemann, *Electrochim. Acta* **2022**, *403*, 139670.
[19] J. Klemens, L. Schneider, D. Burger, N. Zimmerer, M. Müller, W. Bauer, H. Ehrenberg, P. Scharfer, W. Schabel, *Energy Technol.* **2023**, *11*, 2300338.
[20] Z. Wang, A. Hofmann, T. Hanemann, *Electrochim. Acta* **2019**, *298*, 960.
[21] a) B. Han, Y. Zou, Z. Zhang, X. Yang, X. Shi, H. Meng, H. Wang, K. Xu, Y. Deng, M. Gu, *Nat. Commun.* **2021**, *12*, 3066; b) M. Han, C. Zhu, T. Ma, Z. Pan, Z. Tao, J. Chen, *Chem. Commun.* **2018**, *54*, 2381; c) A. Nimkar, N. Shpigel, F. Malchik, S. Bublil, T. Fan, T. R. Penki, M. N. Tsubery, D. Aurbach, *ACS Appl. Mater. Interfaces* **2021**, *13*, 46478.
[22] a) K. Pan, H. Lu, F. Zhong, X. Ai, H. Yang, Y. Cao, *ACS Appl. Mater. Interfaces* **2018**, *10*, 39651; b) A. Ponrouch, A. R. Goñi, M. R. Palacín, *Electrochem. Commun.* **2013**, *27*, 85.
[23] E. Irisarri, A. Ponrouch, M. R. Palacin, *J. Electrochem. Soc.* **2015**, *162*, A2476-A2482.

Manuscript received: July 19, 2023
Revised manuscript received: August 22, 2023
Accepted manuscript online: September 11, 2023
Version of record online: September 28, 2023